Accepted Manuscript

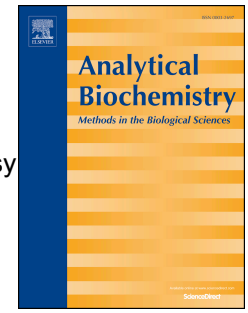

Interfacial electron transfer of glucose oxidase on poly-(glutamic acid)-modified glassy carbon electrode and glucose sensing

Xuechou Zhou, Bingcan Tan, Xinyu Zheng, Dexian Kong, QingLu Li

PII: S0003-2697(15)00383-8

DOI: 10.1016/j.ab.2015.08.007

Reference: YABIO 12161

To appear in: *Analytical Biochemistry*

Received Date: 13 July 2015

Revised Date: 6 August 2015

Accepted Date: 6 August 2015

Please cite this article as: X. Zhou, B. Tan, X. Zheng, D. Kong, Q. Li, Interfacial electron transfer of glucose oxidase on poly-(glutamic acid)-modified glassy carbon electrode and glucose sensing, *Analytical Biochemistry* (2015), doi: 10.1016/j.ab.2015.08.007.

Interfacial electron transfer of glucose oxidase on poly-(glutamic acid)-modified glassy carbon electrode and glucose sensing

Xuechou Zhou [a*], Bingcan Tan [a], Xinyu Zheng [a], Dexian Kong [a], QingLu Li [a,b*]

[a] School of Life Sciences, Fujian Agriculture and Forestry University, Fuzhou, 350002, China.

[b] Engineering Laboratory of Animal Pharmaceuticals, Fujian Province, 350002, China.

[*] E-mail: zhou1300222@outlook.com (X Zhou), lql3388@126.com (Q Li), Fax: +86 591 8378 9155.

Subject category: Enzymatic assays and analyses

Short title: Electron transfer of glucose oxidase and sensing

[*] Corresponding author: zhou1300222@outlook.com (X Zhou), lql3388@126.com (Q Li). Fax: +86 591 8378 9155.

Abstract:

The interfacial electron transfer of glucose oxidase (GOx) on a poly-(glutamic acid)-modified glassy carbon electrode (PGA/GCE) was investigated. The redox peaks measured for GOx and flavin adenine dinucleotide (FAD) are similar, and the anodic peak of GOx does not increase in the presence of glucose in a mediator-free solution. These indicate that the electroactivity of GOx is not the direct electron transfer (DET) between the GOx and PGA/GCE, and the observed electroactivity of GOx is ascribed to free FAD which is released from GOx. However, efficient electron transfer occurred if an appropriate mediator was placed in solution suggesting that the GOx is active. The PGA/GCE based biosensor showed wide linear response in the range of 0.5 – 5.5 mM with a low detection limit of 0.12 mM and high sensitivity and selectivity for measuring glucose.

Keywords: Poly-(glutamic acid)-modified electrode, Glucose oxidase, Interfacial electron transfer, Glucose sensing.

1. Introduction

Glucose oxidase (GOx) has been extensively used to detect the blood glucose levels in diabetics due to its high catalytic ability in glucose oxidation. It enables the electron to transfer from glucose to glucolactone [1]. Since Clark and Lyons firstly proposed the concept of GOx electrode in 1962 [2], researchers have paid great attention to the development of glucose sensors based on the GOx electrodes [3-9]. However, the direct electron transfer between the GOx and electrode surface is difficult to be achieved because the electro-active centers of the GOx are deeply embedded within the protein shells [10]. So, to study of electron transfer between the GOx and electrode surface is considered to be the prerequisite for designing glucose sensor [11]. In the first and second-generation glucose sensors, the electron transfer between the GOx and electrode surface was realized through electron acceptors, such as oxygen, ferrocene derivatives, ferricyanide, p-Acetamidophenol and quinone compounds [12, 13]. Now, many attempts have been made to realize the direct electron transfer (DET) of GOx on the electrode. In this case, it can eliminate the mediator and develop a third-generation glucose sensor with a low operating potential, which is close to that of the redox potential of the enzyme [3].

However, the DET is not a common phenomenon. The DET-based glucose sensor has also been controversial since it depends on the specific conditions and setups of the experiments [14, 15]. Despite a large number of publications suggesting that the GOx can undergo DET on modified electrodes, such as ZnO nanotubes [16], nanostructured gold [17], carbon ionic liquid electrode [18], mesoporous carbon

FDU-15 [19], carbon paste [20, 21], graphene modified electrode [10, 22-24], carbon nanotubes [25-27], three-dimensional porous zirconium phosphate–carbon aerogel composite [28], TiO_2–graphene/nickel oxide nanocomposite [29], multi-walled carbon nanotubes/gold nanorods composite modified electrode [30]，multi-walled carbon nanotubes synthesized on platinum electrode[31] and poly-phenanthroline modified glassy carbon electrode [32]. But, there is only a little of publications[31] which undergoing the DET. On the most of above researches, the DET does not occur and the electron acceptors were also used for the sensor fabricating [14, 15].

Glutamic acid is a well-known amino acid, which can be easily electropolymerized on electrode surface to form a poly-(glutamic acid) (PGA) film [33]. PGA polymer can not only provide the conducting bridges but also promote the electron transfer [34-36]. In this study, the interfacial electron transfer of GOx on a PGA-modified glassy carbon electrode (PGA/GCE) and glucose sensing were investigated. Our results show that the electroactivity of GOx is not the DET between active GOx and PGA/GCE. The anodic peak of GOx does not increase in the presence of glucose in a mediator-free solution. However, the efficient electron transfer occurred if an appropriate electron mediator (quinhydrone or oxygen) was placed in solution.

2. Experimental

2.1 Apparatus

CHI660D Electrochemical Workstation (Shanghai Chenhua Instruments, Shanghai, China) was used for electrochemical measurements. The working electrode

was a glassy carbon electrode (GCE) with a diameter of 3.0 mm, the auxiliary electrode was a platinum wire and the reference electrode was a saturated calomel electrode (SCE).

2.2 Chemicals

Flavin adenine dinucleotide disodium salt hydrate (⩾95%), glucose oxidase (Type X-S from Aspergillus niger 100000−250000 U/g) were purchased from Sigma-Aldrich. All other reagents were bought from local commercial sources with analytical grade. 0.2 M Na_2HPO_4 and 0.2 M NaH_2PO_4 solutions were mixed to form a phosphate buffer solution (0.2 M). Distilled water was used for preparation of all solutions and washing. Both standard and buffer solutions were kept in a refrigerator at 4 ℃.

2.3 Preparation of modified electrodes

The PGA/GCE was constructed by electropolymerization of glutamic acid on the surface of GCE in a solution which contains 0.01 M glutamic acid and 0.1 M phosphate buffer solution (pH = 7.0) by potentiodynamic conditions (12 cycles) in the potential range from -0.5 to 2.0 V at a scan rate of 100 mV s^{-1} [37]. After electropolymerization, the PGA/GCE was washed with distilled water to remove residual monomer. The Cs-GOx-PGA/GCE was prepared by drop casting 2 μL GOx solution (10 mg mL^{-1}) on the PGA/GCE surface. Subsequently, 2 μL of chitosan (Cs) solutions (0.1%, w %) was dropped on the surface of modified electrode to avoid shedding of bound GOx and dried at room temperature. The Cs-FAD-PGA/GCE was prepared by drop casting 2 μL flavin adenine dinucleotide (FAD) solution (10 μM) on

the PGA/GCE surface. Then, 2 μL of chitosan (Cs) solutions (0.1%, w %) was dropped on the surface of modified electrode and dried at room temperature. They were stored at 4 °C before further experiments.

3. Results and discussion

3.1 Interfacial electron transfer of GOx on PGA/GCE

Fig. 1 shows cyclic voltammograms (CVs) of different electrodes in a 0.2 M nitrogen-saturated phosphate buffer solution (pH = 7.0) at a scan rate of 0.1 V s^{-1}. No obvious redox peak was observed when the PGA/GCE was employed (Fig. 1 curve a). A pair of current peaks was observed when the Cs-GOx-PGA/GCE and Cs-FAD-PGA/GCE were employed (Fig. 1 curve b and c). Compared with the CVs of the Cs-GOx-PGA/GCE and Cs-FAD-PGA/GCE, it is found that the redox peaks of them are similar. This suggests that the observed electroactivity of the adsorbed GOx is ascribed to free FAD which is released from GOx [14]. Typically, when the GOx is adsorbed on an electrode some of it denatures, releasing FAD [15].

In order to further confirm the interfacial electron transfer of GOx on PGA/GCE, Fig. 2A shows CVs of the Cs-GOx-PGA/GCE in 0.2 M nitrogen-saturated phosphate buffer solutions (pH = 7.0) with successively adding glucose. It can be seen that the addition of glucose to a nitrogen-saturated solution had no effect on the electroactivity of the Cs-GOx-PGA/GCE, even at a relatively high glucose concentration (5 mM). If the DET occurs, GOx will oxidize glucose and be directly recycled at the electrode surface with no need for any mediator. The glucose should spontaneously reduce FAD, making the reduction peak current decrease, and the oxidation peak current increase.

The lack of sensitivity to glucose clearly indicated that the current peaks at -0.50 V were due to the electroactivity of free FAD that is released from GOx [14]. Even though no change is observed, the GOx is still active and can be verified if an electron mediator is present. Fig. 2B shows the CVs of Cs-GOx-PGA/GCE in 0.2 M air-saturated phosphate buffer solutions (pH = 7.0) without and with the addition of various concentrations of glucose at a scan rate of 0.1 V s^{-1}. The addition of glucose to an air-saturated solution resulted in the shift of the entire voltammogram toward lower cathodic currents. The shift was ascribed to the decrease of O_2 reduction current due to the depletion of O_2 in a biosensor by the mediated enzymatic process. In addition, the shift did not affect the background-corrected current peaks at −0.5 V. It indicates that the FAD peak does not change and the DET is not occurring between GOx and PGA/GCE. This phenomenon can be further verified by using quinhydrone (QH) as electron mediator. Fig. 2C shows CVs of Cs-GOx-PGA/GCE in 0.2 M nitrogen-saturated phosphate buffer solutions (pH = 7.0) containing 0.3 mM QH at a scan rate of 0.1 V s^{-1} before and after successively adding 0.5 mM glucose. It can be seen that a pair of well-defined redox peaks occurred (curve a) in the absence of glucose. The peaks correspond to the redox reaction of QH. An increase in anodic peak current and decrease in cathodic peak current were observed with the addition of glucose (curve b - i). It is ascribed to the interaction between QH and GOx($FADH_2$), which was formed in catalytic reaction. This can be explained by the equations (1 - 3):

$$\mathrm{GOx(FAD)} + \mathrm{Glucose} \rightarrow \mathrm{GOx(FADH_2)} + \mathrm{Gluconolactone} \quad (1)$$

$$\mathrm{GOx(FADH_2)} + \mathit{Q}\mathrm{H} \rightarrow \mathrm{GOx(FAD)} + \mathit{Q}\mathrm{H(H_2)} \quad (2)$$

$$QH(H_2) \rightarrow QH + 2e^- + 2H^+ \quad (3)$$

Figure 2D and E display CVs of the Cs-FAD-PGA/GCE in phosphate buffer solutions containing different electron mediator before and after successively adding 0.5 mM glucose, which do not show enzymatic activity as a function of the glucose concentration in the presence of air or QH.

The effect of scan rate on the peak currents of the Cs-GOx-PGA/GCE and Cs-FAD-PGA/GCE is shown in Fig. 3. The anodic and cathodic peak currents of the Cs-GOx-PGA/GCE increased linearly when the scan rate was increased from 0.02 to 0.7 V s^{-1} (as shown in Fig. 3C), which is a characteristic of a surface-controlled process. The electron-transfer-rate constant (k_s) of of the Cs-GOx-PGA/GCE can be estimated using the Laviron's model [38]. Plots of the E_{pa} and E_{pc} vs. the logarithm of the scan rates produce two straight lines with slopes of $2.3RT/(1-\alpha)nF$ and $-2.3RT/\alpha nF$ at high scan rates (Fig. 3E). From the slopes, α is estimated to be 0.44. The average electron transfer rate constant k_s of the Cs-GOx-PGA/GCE was estimated to be 11.0 s^{-1} by using the formula [38] below:

$$k_s = \frac{mnFv}{RT} \quad (4)$$

Here m is a parameter related to the peak-to-peak separation, F is Faraday's constant, R is the gas constant, T is the temperature, n is the number of electrons transferred, and v is the scan rate. The anodic and cathodic peak currents of the Cs-FAD-PGA/GCE also increased linearly when the scan rate was increased from 0.02 to 0.7 V s^{-1} (as shown in Fig. 3D). The average electron transfer rate constant k_s of the Cs-FAD-PGA/GCE was estimated to be 10.7 s^{-1} when the above method was

employed. The obtained value is larger than these values observed for GOx immobilized on some other materials [18, 21, 32].

In order to determine the effect of pH value on the Cs-GOx-PGA/GCE and Cs-FAD-PGA/GCE, the CVs were recorded in a 0.2 M nitrogen-saturated phosphate buffer solutions at different pH values (Fig. 4). It is found that the E^0 of Cs-GOx-PGA/GCE and Cs-FAD-PGA/GCE has a linear relativity to the buffer pH values with a slope of 58.4 and 58.0 mV/pH, respectively (Fig. 4C and D). These values are basically the same as the theoretical value of 58.6 mV/pH [39] with two-electron and two-proton transportation.

These results indicate that the electroactivity of GOx is not the direct electron transfer (DET) between the GOx and PGA/GCE, and the observed electroactivity of GOx is ascribed to free FAD which is released from GOx. The GOx molecules immobilized on PGA/GCE still maintain its catalytic activity towards glucose oxidation. Similar phenomenon at other modified electrodes has been recently reported [14, 15].

3.2 Mediated Detection of Glucose at the Cs-GOx-PGA/GCE based biosensor

Based on the above results, the DET from enzyme-active FAD on the Cs-GOx-PGA/GCE is not observed when the glucose is added to a mediator-free solution. So, an appropriate electron mediator must be placed in solution in the case of glucose detection. Oxygen is a natural electron mediator. In the first generation of glucose sensor, the electron transfer between the GOx and electrode surface was realized through oxygen. This kind of biosensor may involve the following reactions:

$$GOx(FAD) + Glucose \rightarrow GOx(FADH_2) + Gluconolactone \quad (5)$$

$$GOx(FADH_2) + O_2 \rightarrow GOx(FAD) + H_2O_2 \quad (6)$$

$$H_2O_2 \rightarrow O_2 + 2e^- + 2H^+ \quad (7)$$

The concentration of glucose was determined by the oxidation of H_2O_2 that was produced by the sequence of reaction 7.

In this study, the concentration of glucose was determined by the decrease in O_2 reduction current in air-saturated solution. According to the reaction Equations 5 and 6, there is a linear relationship between the amount of glucose and consumed O_2. So, it is possible to fabricate an amperometric glucose biosensor in which the decrease of concentration of dissolved O_2 is monitored to indicate the concentration of glucose [3]. The O_2 consumption can be detected by the electrode according to the following Equation：

$$O_2 + 4H^+ + 4e^- \rightarrow 2H_2O \quad (8)$$

Fig. 5 displays the amperometric response of the Cs-GOx-PGA/GCE in 0.2 M air-saturated phosphate buffer solutions (pH = 7.0) at the different applied potential with consecutive addition of 0.5 mM glucose. The current response to glucose is increasing with the decrease of the applied potential, but the i-t curve exhibits unclear step at high glucose concentration when the potential was applied at −0.4 V. Therefore, glucose measurements were performed at the potential of −0.35 V.

The relation between current and glucose concentration under the optimized experimental conditions is illustrated in Fig. 6. The reduction peak current decreased after each addition of glucose to the stirred air-saturated phosphate buffer solutions.

The curve of the Cs-GOx-PGA/GCE exhibits clear steps with successive increase of the glucose concentration. However, the i-t curve of the Cs-GOx/GCE shows unclear steps in high glucose concentration. This indicates that the PGA precursor can protect denature of glucose oxidase. An enzyme binding directly on an electrode surface would be easily denatured in comparison with an enzyme binding on precursor modified electrode[40]. In addition, the PGA contains glutamate repeat units and free protonated carboxylic groups (pKa = 4.45) by linking the α-amino and δ-carboxylic acid functional groups [34], so it can not only provide the conducting bridges but also promote the electron transfer. The response current of the Cs-GOx-PGA/GCE is linear with respect to the glucose concentration in the range of 0.5 – 5.5 mM, with a regression coefficient of 0.998 and a detection limit of 0.12 mM (S/N = 3). From the slope, the sensitivity of the biosensor was calculated to be 2.13 μ A mM−1 cm−2. To demonstrate the advantages of the prepared Cs-GOx-PGA/GCE glucose sensor, we compared with the performance of the reported enzyme glucose sensors. As listed in Table 1, the applied potential, detection limit, linear calibration range and sensitivity for glucose determination at the Cs-GOx-PGA/GCE were comparable or even better than those obtained at several electrodes reported recently [6, 41-48]. In addition, the fabrication process of the Cs-GOx-PGA/GCE glucose sensor was simple and facile.

The effect of possible interfering species such as uric acid (UA), fructose, p-acetamidophenol (AP) and ascorbic acid (AA) was also examined. The physiological level of glucose is at least 30 times higher than that of the interfering species [49]. Therefore, the interfering species were tested by adding a concentration

of 0.02 mM or 0.1 mM. Fig. 7 shows the response of the Cs-GOx-PGA/GCE to glucose upon addition of 0.5 mM fructose, 0.1 mM AA, 0.02 mM UA and 0.1 mM AP. It was observed that the response signals of fructose, AA, UA and AP are negligible for glucose determination at the Cs-GOx-PGA/GCE under the present conditions. These results suggest that the proposed Cs-GOx-PGA/GCE has high selectivity due to the low operating potential (−0.35 V).

The operational stability of the Cs-GOx-PGA/GCE was examined by successive detection of 0.5 mM glucose for 5 times. The relative standard deviations (RSD) were found to be 2.8%. The performance of the Cs-GOx-PGA/GCE does not change obviously when it was placed at 4 °C in a refrigerator. After placing for three weeks, the current response still retains 90.5% of its initial current response. It demonstrates that the Cs-GOx-PGA/GCE shows good stability.

Under the optimum conditions, glucose injection sample was selected for sample analysis using the standard addition method. Glucose injection samples (250 ml: 12.5 g) were obtained from local hospital and diluted with 0.2 M PBS to fit into the linear range. A rapid and stable amperometric response was acquired at -0.35V with the addition of 100 μL of sample into 20.0 mL of 0.2 M PBS. After the current responses were determined, different concentration of glucose standard samples were successively added into the system for standard addition determination. The obtained results are shown in Table 2. The results show that the proposed sensor could be efficiently used for the determination of glucose in practical samples.

4. Conclusions

The interfacial electron transfer of the GOx on PGA/GCE and glucose sensing were investigated by cyclic voltammetry and chronoamperomtery. The redox peaks measured for GOx and FAD are similar, and the anodic peak of GOx does not increase in the presence of glucose in a mediator-free solution. These indicate that the electroactivity of GOx is not DET between the GOx and PGA/GCE, and the observed electroactivity of GOx is from free FAD. However, the GOx is active, clearly shown if an electron mediator is employed. In the presence of oxygen, the Cs-GOx-PGA/GCE displays the desirable analytical performance with a wide linear range, low detection limit and excellent selectivity for measuring glucose. Therefore, the PGA/GCE is a good material which is promising for construction of enzyme biosensor and bioelectrochemical devices.

Acknowledgements

The authors are grateful for the Scientific Research Fund of Fujian Provincial Education Department (JA13106).

References

[1] Z. Dai, J. Ni, X. Huang, G. Lu, J. Bao, Direct electrochemistry of glucose oxidase immobilized on a hexagonal mesoporous silica-MCM-41 matrix, Bioelectrochemistry, 70 (2007) 250-256.

[2] L.C. Clark, C. Lyons, Electrode systems for continuous monitoring in cardiovascular surgery, Annals of the New York Academy of sciences, 102 (1962) 29-45.

[3] J. Wang, Glucose biosensors: 40 years of advances and challenges, Electroanalysis, 13 (2001) 983.

[4] C. Chen, Q. Xie, D. Yang, H. Xiao, Y. Fu, Y. Tan, S. Yao, Recent advances in electrochemical glucose biosensors: a review, Rsc Advances, 3 (2013) 4473-4491.

[5] W.T. Shi, J. Di, Z.F. Ma, Electrochemical Glucose Biosensors, Prog. Chem., 24 (2012) 568-576.

[6] N. German, A. Ramanavicius, A. Ramanaviciene, Electrochemical deposition of gold nanoparticles on graphite rod for glucose biosensing, Sensors and Actuators B: Chemical, 203 (2014) 25-34.

[7] M.Y. Elahi, A. Khodadadi, Y. Mortazavi, A glucose biosensor based on glucose oxidase immobilized on ZnO/Cu2O graphene oxide nanocomposite electrode, Journal of The Electrochemical Society, 161 (2014) B81-B87.

[8] J. Hui, J. Cui, Y. Wang, Y. Zhang, J. Liang, X. Zhang, W. Chen, E.E. Ogabiela, S.B. Adeloju, Y. Wu, A High Throughput Glucose Biosensor Based on FIA and Gold Nanowire Arrays at Low Potential, Journal of The Electrochemical Society, 161 (2014) B291-B296.

[9] E. Zor, Y. Oztekin, A. Ramanaviciene, Z. Anusevicius, H. Bingol, J. Barkauskas, M. Ersoz, A. Ramanavicius, Amperometric Glucose Biosensor Based on Glucose Oxidase, 1, 10-Phenanthroline-5, 6-dione and Carbon Nanotubes, Journal of The Electrochemical Society, 161 (2014) H3064-H3069.

[10] C. Fu, W. Yang, X. Chen, D.G. Evans, Direct electrochemistry of glucose oxidase on a graphite nanosheet–Nafion composite film modified electrode, Electrochemistry Communications, 11 (2009) 997-1000.

[11] X. Xu, J. Chen, W. Li, Z. Nie, S. Yao, Surface nanocrystallization of glassy carbon electrode: Application in direct electrochemistry of glucose oxidase, Electrochemistry Communications, 10 (2008) 1459-1462.

[12] A.E. Cass, G. Davis, G.D. Francis, H.A.O. Hill, W.J. Aston, I.J. Higgins, E.V. Plotkin, L.D. Scott, A.P. Turner, Ferrocene-mediated enzyme electrode for amperometric determination of glucose, Analytical chemistry, 56 (1984) 667-671.

[13] T. Kohma, H. Kitajima, D. Oyamatsu, S. Kuwabata, Glucose sensing using p-acetamidophenol as an electron mediator between glucose oxidase and nafion-coated glassy carbon electrode, Electrochemistry, 74 (2006) 804-809.

[14] M. Wooten, S. Karra, M. Zhang, W. Gorski, On the direct electron transfer, sensing, and enzyme activity in the glucose oxidase/carbon nanotubes system, Analytical chemistry, 86 (2013) 752-757.

[15] J.M. Goran, S.M. Mantilla, K.J. Stevenson, Influence of surface adsorption on the interfacial electron transfer of flavin adenine dinucleotide and glucose oxidase at carbon nanotube and nitrogen-doped carbon nanotube electrodes, Analytical chemistry, 85 (2013) 1571-1581.

[16] T. Kong, Y. Chen, Y. Ye, K. Zhang, Z. Wang, X. Wang, An amperometric glucose biosensor based on the immobilization of glucose oxidase on the ZnO nanotubes, Sensors and Actuators B: Chemical, 138 (2009) 344-350.

[17] C. Qiu, X. Wang, X. Liu, S. Hou, H. Ma, Direct electrochemistry of glucose oxidase immobilized on nanostructured gold thin films and its application to bioelectrochemical glucose sensor, Electrochimica Acta, 67 (2012) 140-146.

[18] X. Shangguan, H. Zhang, J. Zheng, Direct electrochemistry of glucose oxidase based on its direct immobilization on carbon ionic liquid electrode and glucose sensing, Electrochemistry Communications, 10 (2008) 1140-1143.

[19] K. Wang, H. Yang, L. Zhu, Z. Ma, S. Xing, Q. Lv, J. Liao, C. Liu, W. Xing, Direct electron transfer and electrocatalysis of glucose oxidase immobilized on glassy carbon electrode modified with Nafion and mesoporous carbon FDU-15, Electrochimica Acta, 54 (2009) 4626-4630.

[20] D. Savitri, C.K. Mitra, Electrochemistry of reconstituted glucose oxidase on carbon paste electrodes, Bioelectrochemistry and bioenergetics, 47 (1998) 67-73.

[21] S. Liu, H. Ju, Reagentless glucose biosensor based on direct electron transfer of glucose oxidase immobilized on colloidal gold modified carbon paste electrode, Biosensors and Bioelectronics, 19 (2003) 177-183.

[22] M. Cui, B. Xu, C. Hu, H.B. Shao, L. Qu, Direct electrochemistry and electrocatalysis of glucose oxidase on three-dimensional interpenetrating, porous graphene modified electrode, Electrochimica Acta, 98 (2013) 48-53.

[23] B. Liang, L. Fang, G. Yang, Y. Hu, X. Guo, X. Ye, Direct electron transfer glucose biosensor based on glucose oxidase self-assembled on electrochemically reduced carboxyl graphene, Biosensors and Bioelectronics, 43 (2013) 131-136.

[24] P. Wu, Q. Shao, Y. Hu, J. Jin, Y. Yin, H. Zhang, C. Cai, Direct electrochemistry of glucose oxidase assembled on graphene and application to glucose detection, Electrochimica Acta, 55 (2010) 8606-8614.

[25] C. Cai, J. Chen, Direct electron transfer of glucose oxidase promoted by carbon nanotubes, Analytical biochemistry, 332 (2004) 75-83.

[26] M.V. Jose, S. Marx, H. Murata, R.R. Koepsel, A.J. Russell, Direct electron transfer in a mediator-free glucose oxidase-based carbon nanotube-coated biosensor, Carbon, 50 (2012) 4010-4020.

[27] Q. Gao, Y. Guo, J. Liu, X. Yuan, H. Qi, C. Zhang, A biosensor prepared by co-entrapment of a glucose oxidase and a carbon nanotube within an electrochemically deposited redox polymer multilayer, Bioelectrochemistry, 81 (2011) 109-113.

[28] Z. Yu, Y. Kou, Y. Dai, X. Wang, H. Wei, D. Xia, Direct Electrochemistry of Glucose Oxidase on a Three-Dimensional Porous Zirconium Phosphate–Carbon Aerogel Composite, Electrocatalysis, (2015) 1-7.

[29] C.-X. Xu, K.-J. Huang, X.-M. Chen, X.-Q. Xiong, Direct electrochemistry of glucose oxidase immobilized on TiO2–graphene/nickel oxide nanocomposite film and its application, Journal of Solid State Electrochemistry, 16 (2012) 3747-3752.

[30] Y. Li, F. Wang, F. Huang, Y. Li, S. Feng, Direct electrochemistry of glucose oxidase and its biosensing to glucose based on the Chit-MWCNTs–AuNRs modified gold electrode, Journal of Electroanalytical Chemistry, 685 (2012) 86-90.

[31] M. Tominaga, S. Nomura, I. Taniguchi, Bioelectrocatalytic current based on direct heterogeneous electron transfer reaction of glucose oxidase adsorbed onto multi-walled carbon nanotubes synthesized on platinum electrode surfaces, Electrochemistry Communications, 10 (2008) 888-890.

[32] Y. Oztekin, A. Ramanaviciene, Z. Yazicigil, A.O. Solak, A. Ramanavicius, Direct electron transfer from glucose oxidase immobilized on polyphenanthroline-modified glassy carbon electrode, Biosensors and Bioelectronics, 26 (2011) 2541-2546.

[33] D.P. Santos, M.V.B. Zanoni, M.F. Bergamini, A.-M. Chiorcea-Paquim, V.C. Diculescu, A.-M.O. Brett, Poly (glutamic acid) nanofibre modified glassy carbon electrode: Characterization by atomic

force microscopy, voltammetry and electrochemical impedance, Electrochimica Acta, 53 (2008) 3991-4000.

[34] X. Liu, L. Luo, Y. Ding, D. Ye, Poly-glutamic acid modified carbon nanotube-doped carbon paste electrode for sensitive detection of L-tryptophan, Bioelectrochemistry, 82 (2011) 38-45.

[35] A.-M. Yu, H.-Y. Chen, Electrocatalytic oxidation and determination of ascorbic acid at poly (glutamic acid) chemically modified electrode, Analytica chimica acta, 344 (1997) 181-185.

[36] Y. Zhang, L. Luo, Y. Ding, X. Liu, Z. Qian, A highly sensitive method for determination of paracetamol by adsorptive stripping voltammetry using a carbon paste electrode modified with nanogold and glutamic acid, Microchimica Acta, 171 (2010) 133-138.

[37] X. Zhou, X. Zheng, R. Lv, D. Kong, Q. Li, Electrodeposition of platinum on poly (glutamic acid) modified glassy carbon electrode for non-enzymatic amperometric glucose detection, Electrochimica Acta, 107 (2013) 164-169.

[38] E. Laviron, General expression of the linear potential sweep voltammogram in the case of diffusionless electrochemical systems, Journal of Electroanalytical Chemistry and Interfacial Electrochemistry, 101 (1979) 19-28.

[39] Y. Huang, W. Zhang, H. Xiao, G. Li, An electrochemical investigation of glucose oxidase at a CdS nanoparticles modified electrode, Biosensors and Bioelectronics, 21 (2005) 817-821.

[40] Y. Sugimoto, Y. Kitazumi, S. Tsujimura, O. Shirai, M. Yamamoto, K. Kano, Electrostatic interaction between an enzyme and electrodes in the electric double layer examined in a view of direct electron transfer-type bioelectrocatalysis, Biosensors and Bioelectronics, 63 (2015) 138-144.

[41] S. Tang, X. Wang, J. Lei, Z. Hu, S. Deng, H. Ju, Pt-dispersed flower-like carbon nanosheet aggregation for low-overpotential electrochemical biosensing, Biosensors and Bioelectronics, 26 (2010) 432-436.

[42] X. Ren, D. Chen, X. Meng, F. Tang, A. Du, L. Zhang, Amperometric glucose biosensor based on a gold nanorods/cellulose acetate composite film as immobilization matrix, Colloids and Surfaces B: Biointerfaces, 72 (2009) 188-192.

[43] Y. Wang, L. Liu, M. Li, S. Xu, F. Gao, Multifunctional carbon nanotubes for direct electrochemistry of glucose oxidase and glucose bioassay, Biosensors and Bioelectronics, 30 (2011) 107-111.

[44] Y. Liu, M. Wang, F. Zhao, Z. Xu, S. Dong, The direct electron transfer of glucose oxidase and glucose biosensor based on carbon nanotubes/chitosan matrix, Biosensors and Bioelectronics, 21 (2005) 984-988.

[45] K. Wang, Q. Liu, Q.-M. Guan, J. Wu, H.-N. Li, J.-J. Yan, Enhanced direct electrochemistry of glucose oxidase and biosensing for glucose via synergy effect of graphene and CdS nanocrystals, Biosensors and Bioelectronics, 26 (2011) 2252-2257.

[46] B. Haghighi, M.A. Tabrizi, Direct electron transfer from glucose oxidase immobilized on a nano-porous glassy carbon electrode, Electrochimica Acta, 56 (2011) 10101-10106.

[47] M.a.D. Rubianes, G.A. Rivas, Carbon nanotubes paste electrode, Electrochemistry Communications, 5 (2003) 689-694.

[48] B. Unnikrishnan, S. Palanisamy, S.-M. Chen, A simple electrochemical approach to fabricate a glucose biosensor based on graphene–glucose oxidase biocomposite, Biosensors and Bioelectronics, 39 (2013) 70-75.

[49] Q. Xu, L. Yin, C. Hou, X. Liu, X. Hu, Facile fabrication of nanoporous platinum by alloying–dealloying process and its application in glucose sensing, Sensors Actuators B: Chem., 173

(2012) 716-723.

Tables:

Table 1 Comparison of different enzymatic glucose sensors.

Electrode material	Sensitivity	Linear range	Detection limit
GOx/Au-NPs/graphite [6]	101.02 μA $mM^{-1}cm^{-2}$ (0.3 V)	0.1–10.0 mM	0.083 mM
GOx/Pt/FCNA/GCE[a] [41]	6.0 μA mM^{-1} (-0.08 V)	0.5–8.0 mM	0.3 mM
GOx/Au nanorods/cellulose acetate [42]	8.4 μA mM^{-1} cm^{-2} (0.4 V)	0.03–2.2 mM	0.02 mM
Nafion/GOx/Ag-Pdop@CNT/GCE[b] [43]	3.1 μA mM^{-1} cm^{-2} (-0.5 V)	0.55–1.1 mM	0.017 mM
GOx-CNTs-chitosan/GCE[c] [44]	7.36 μA mM^{-1} cm^{-2} (0.4 V)	0.0–7.8 mM	Not applicable
G–CdS–GOD/GCE [45]	1.74 μA mM^{-1} cm^{-2} (Not applicable)	2–16 mM	0.7 mM
GCE-red/GOx/Nafion [46]	Not applicable (-0.29 V)	1–7 mM	0.1 mM
GOx–CNTPE[d] [47]	11.3 μA mM^{-1} cm^{-2}(-0.1 V)	0–25 mM	0.6 mM
Graphene- GOx [48]	1.85 μA mM^{-1} cm^{-2}(-0.44 V)	0.1–27 mM	Not applicable
This work	2.13 μA mM^{-1} cm^{-2} (-0.35 V)	0.5–5. 5 mM	0.12 mM

[a] Flower-like carbon nanosheet aggregation

[b] Polydopamine

[c] Carbon nanotubes

[d] Carbon nanotubes paste electrodes

Table 2 Determination of Glucose in glucose injection solution samples

Sample	Content / mM	Added / mM	Found / mM	Recovery (%)	RSD (%)
1	1.386	0.25	1.642	102.4	3.05
2	1.386	3.000	4.476	103.0	4.27

Figure captions

Fig. 1 CVs of different electrodes in 0.2 M nitrogen-saturated phosphate buffer solutions (pH = 7.0) at a scan rate of 0.1 V s^{-1} (a=PGA/GCE, b=Cs-GOx-PGA/GCE; c=Cs-FAD-PGA/GCE).

Fig. 2 (A) CVs of the Cs-GOx-PGA/GCE in 0.2 M nitrogen-saturated phosphate buffer solutions (pH = 7.0) at a scan rate of 0.1 V s^{-1} before (a) and after successively adding different concentration of glucose (b=0.5 mM, c=2 mM, d=5 mM). (B) CVs of the Cs-GOx-PGA/GCE in 0.2 M air-saturated phosphate buffer solutions (pH = 7.0) at a scan rate of 0.1 V s^{-1} before (a) and after successively adding 0.5 mM glucose (b - k). (C) CVs of the Cs-GOx-PGA/GCE in 0.2 M nitrogen-saturated phosphate buffer solutions (pH = 7.0) containing 0.3 mM quinhydrone at a scan rate of 0.1 V s^{-1} before (a) and after successively adding 0.5 mM glucose (b - i). (D) CVs of the Cs-FAD-PGA/GCE in 0.2 M air-saturated phosphate buffer solutions (pH = 7.0) at a scan rate of 0.1 V s^{-1} before (a) and after successively adding 0.5 mM glucose (b - d). (E) CVs of the Cs-FAD-PGA/GCE in 0.2 M nitrogen-saturated phosphate buffer solutions (pH = 7.0) containing 0.3 mM quinhydrone at a scan rate of 0.1 V s^{-1} before (a) and after successively adding 0.5 mM glucose (b - d).

Fig. 3 CVs of the Cs-GOx-PGA/GCE (A) and Cs-FAD-PGA/GCE (B) in 0.2 M nitrogen-saturated phosphate buffer solutions (pH = 7.0) with the scan rate of 0.02 – 0.7 V s^{-1}. The linear dependence of anodic peak currents on the Cs-GOx-PGA/GCE (C) and Cs-FAD-PGA/GCE (D) vs. scan rate, and the relationship of the peak potential (E_p) vs. the logarithm of scan rate (E).

Fig. 4 CVs of the Cs-GOx-PGA/GCE (A) and Cs-FAD-PGA/GCE (B) in 0.2 M nitrogen-saturated phosphate buffer solutions at different pH values with a scan rate of 0.1 V s^{-1} (a–e: 8.0, 7.5, 7.0, 6.5 and 6.0). The linear dependence of E^0 on the Cs-GOx-PGA/GCE (C) and Cs-FAD-PGA/GCE (D) vs. pH.

Fig. 5 The amperometric response of the Cs-GOx-PGA/GCE in 0.2 M air-saturated phosphate buffer solutions (pH = 7.0) at the different applied potential with consecutive addition of 0.5 mM glucose (a: - 0.3 V, b: - 0.35 V, c: - 0.4 V).

Fig. 6 (A) The amperometric response of the Cs-GOx/GCE (a) and Cs-GOx-PGA/GCE (b) in 0.2 M air-saturated phosphate buffer solutions (pH = 7.0) at -0.35 V with consecutive addition of 0.5 mM glucose; (B) The corresponding calibration curves of the response current on the Cs-GOx-PGA/GCE vs. glucose concentration.

Fig. 7 Amperometric response of Cs-GOx-PGA/GCE successive addition of 0.50 mM glucose (a), 0.50 mM fructose (b), 0.1 mM AA (c), 0.02 mM UA (d), 0.1 mM AP (e), 0.50 mM glucose (f) in 0.2 M air-saturated phosphate buffer solutions (pH = 7.0) at -0.35 V.

Fig. 1

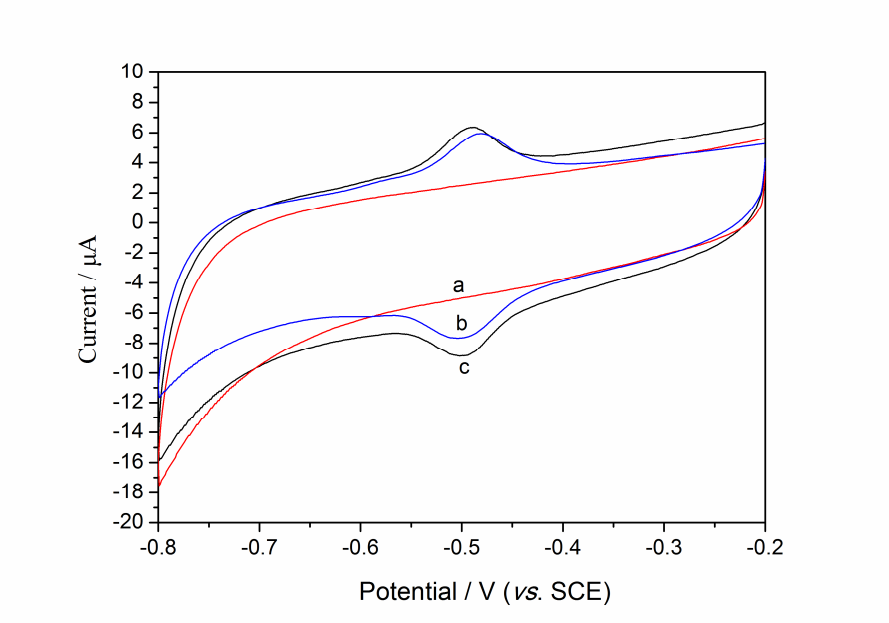

Fig. 2

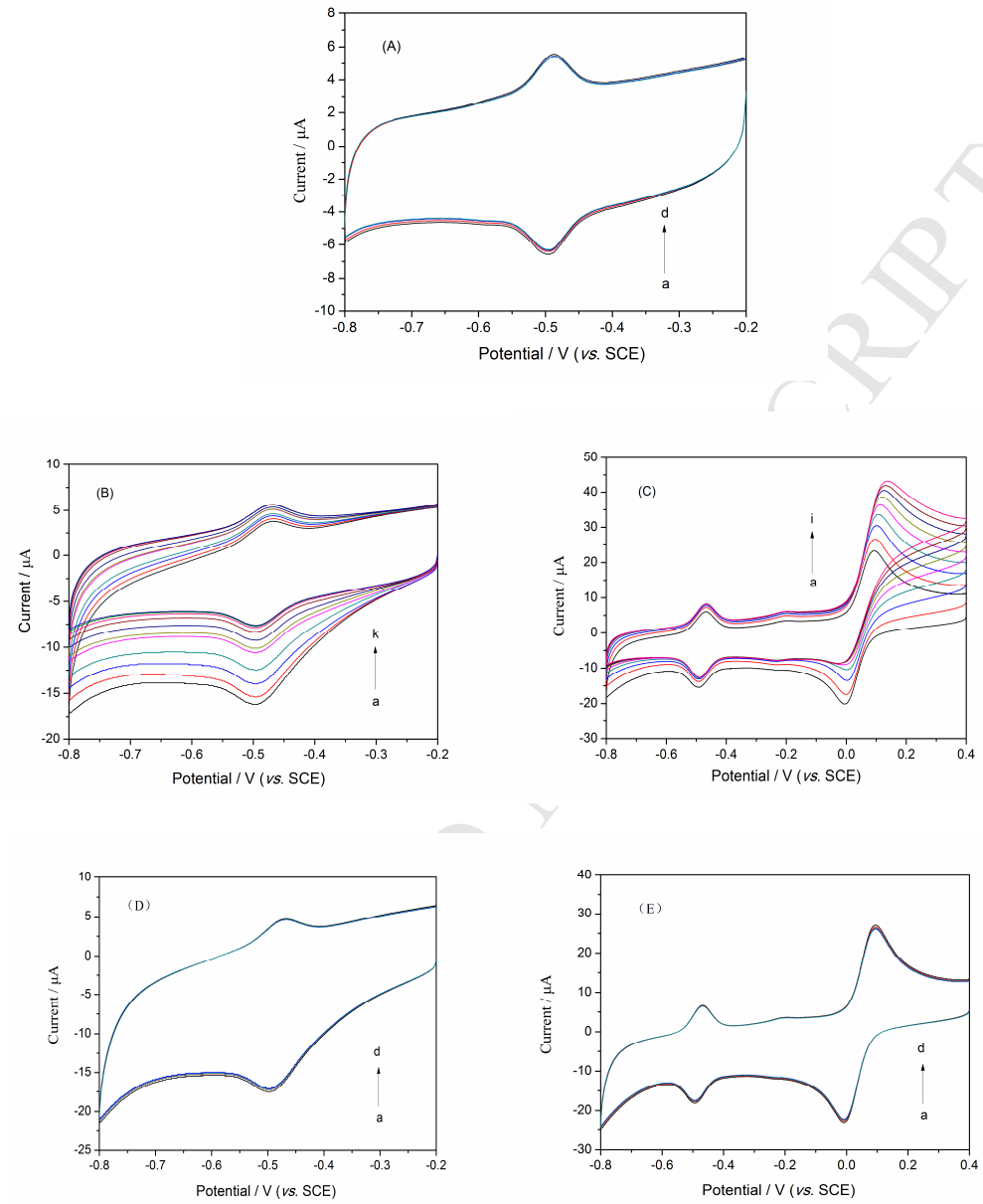
(A)
Current / μA
Potential / V (vs. SCE)
d
a
(B)
Current / μA
Potential / V (vs. SCE)
k
a
(C)
Current / μA
Potential / V (vs. SCE)
i
a
(D)
Current / μA
Potential / V (vs. SCE)
d
a
(E)
Current / μA
Potential / V (vs. SCE)
d
a

Fig. 3

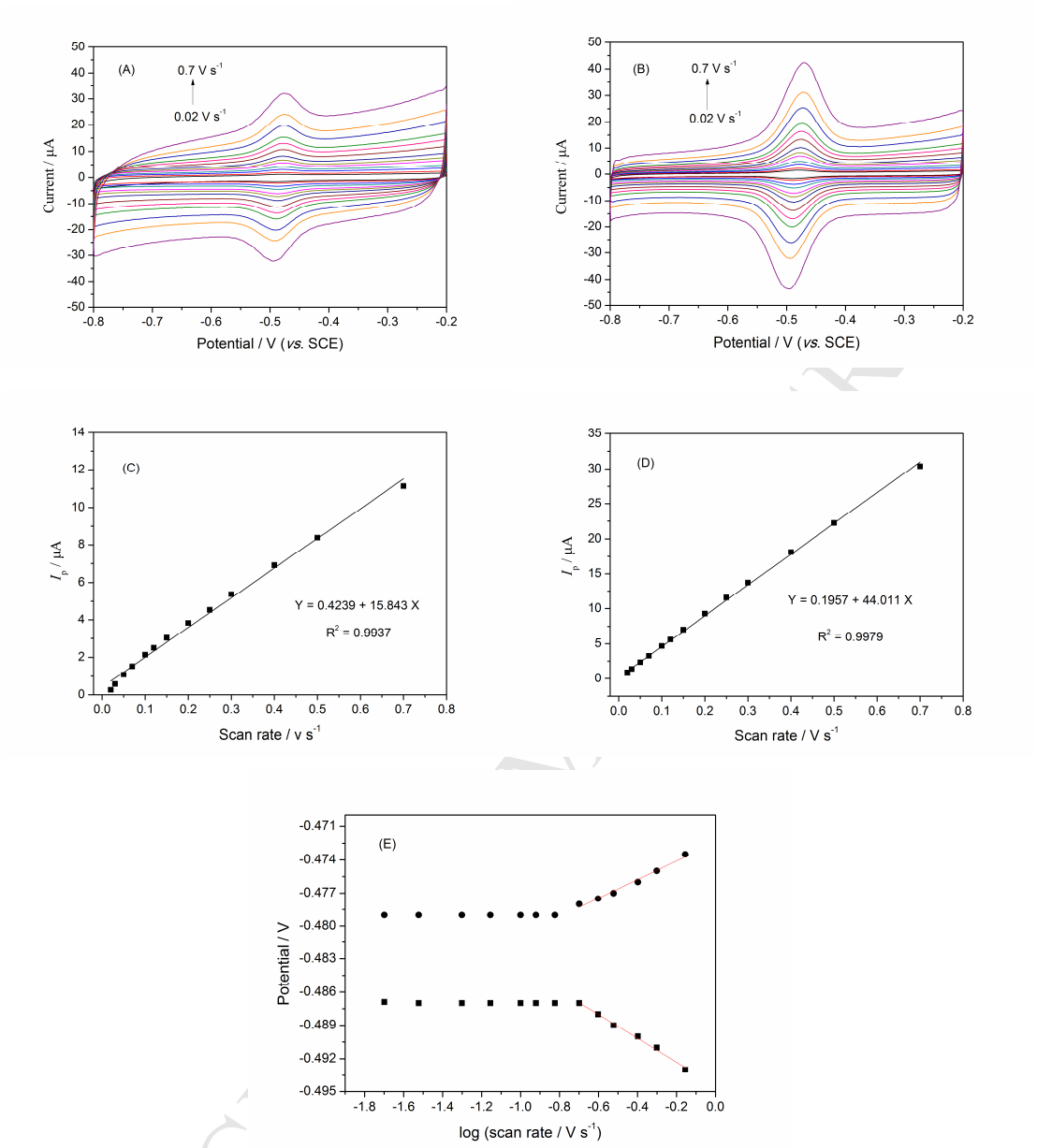
(A)
0.7 V s-1
0.02 V s-1
Current / µA
Potential / V (vs. SCE)
(B)
0.7 V s-1
0.02 V s-1
Current / µA
Potential / V (vs. SCE)
(C)
Y = 0.4239 + 15.843 X
R2 = 0.9937
Ip / µA
Scan rate / v s-1
(D)
Y = 0.1957 + 44.011 X
R2 = 0.9979
Ip / µA
Scan rate / V s-1
(E)
Potential / V
log (scan rate / V s-1)

Fig. 4

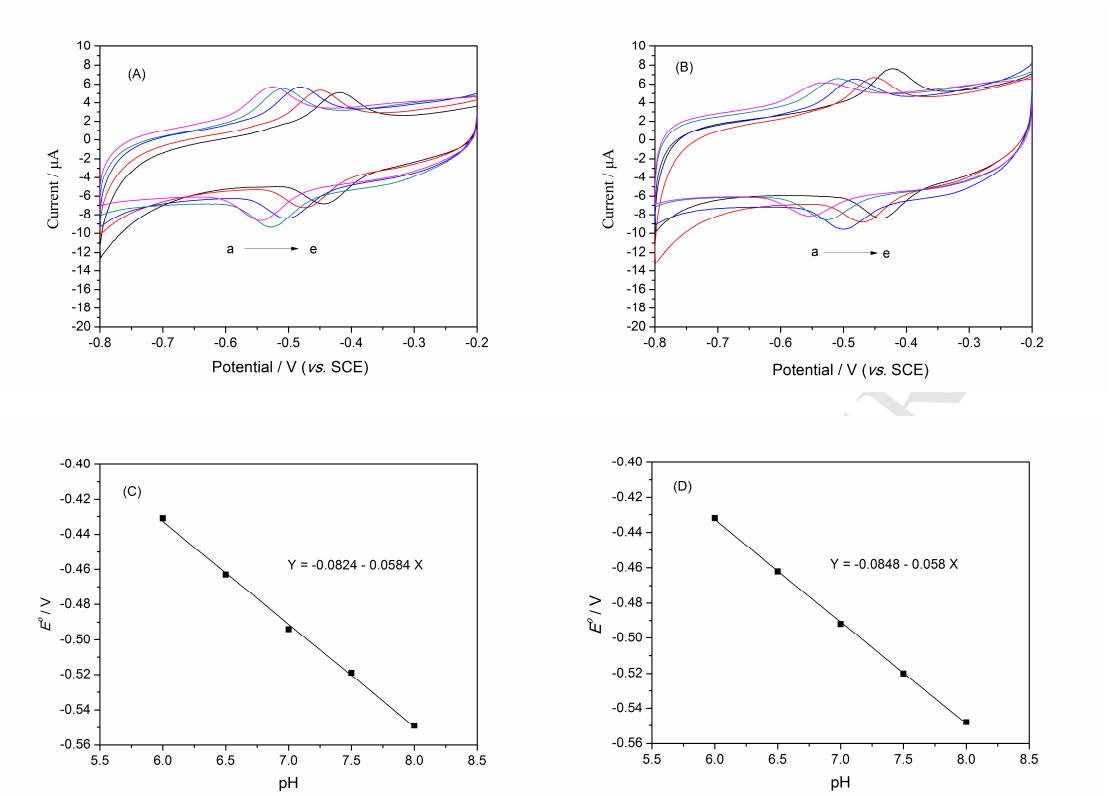

Fig. 5

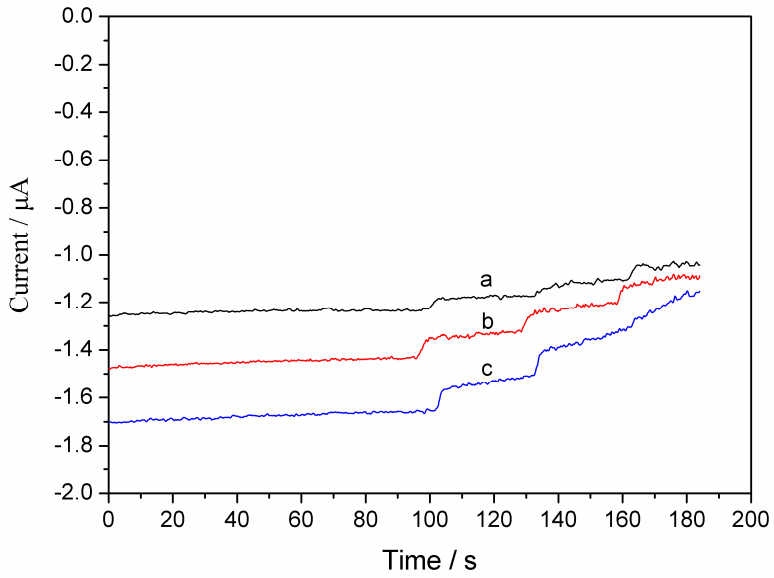

Fig. 6

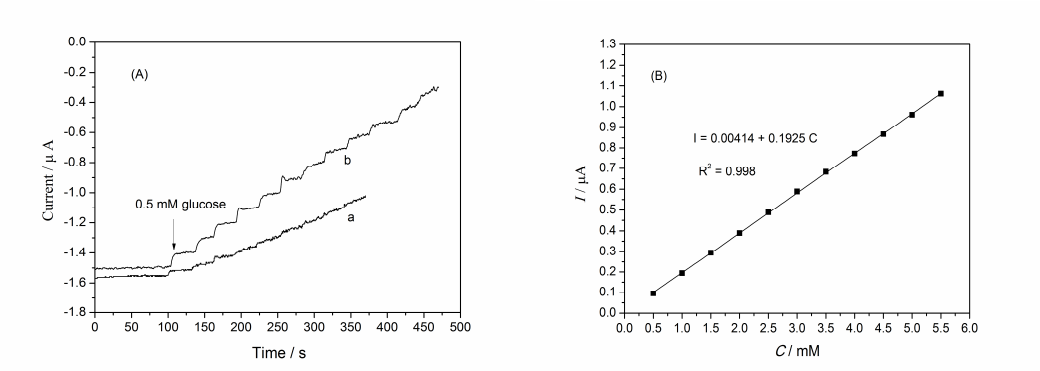

Fig. 7